

# Effect of the Complexing Agent on the Synthesis of $WO_3$ Nanostructures for Energy Storage Applications

Gemma Roselló-Márquez, Dionisio M. García-García, Mireia Cifre-Herrando, José García-Antón

Ingeniería Electroquímica y Corrosión (IEC), Instituto Universitario de Seguridad Industrial, Radiofísica y Medioambiental (ISIRYM), Universitat Politècnica de València, C/Camino de Vera s/n, 46022, Valencia, Spain  
[jgarciaa@iqn.upv.es](mailto:jgarciaa@iqn.upv.es)

Nowadays, energy problems have become one of our society's biggest challenges and have drawn worldwide attention. Rechargeable lithium-ion batteries (LIBs) are a good option to solve these problems thanks to their high energy density and good cycle stability. However, much effort has recently been devoted to find alternative anode materials and replace graphite in LIBs, like tungsten oxide ( $WO_3$ ) which has attracted much interest as an anode due to its excellent properties.

In this work, a simple method is used to synthesize crystalline  $WO_3$  nanostructures, with well-defined morphology using an electrochemical procedure known as electrochemical anodization. This method presents several advantages such as being a simple procedure and easy to control its parameters. During the anodization, two different complexing agents (oxygen peroxide and citric acid) were used. The effect of each complexing agent on the anode behaviour of nanostructures in lithium-ion batteries has been evaluated.

On the one hand, Field Emission Scanning Electron Microscopy (FE-SEM) has been used to study the morphology of the samples, Raman Spectroscopy technique has been employed to verify the composition and crystallinity of the nanostructures and Electrochemical Impedance Spectroscopy (EIS) was performed to study their electrochemical properties.

Finally, the different samples were applied as an anode for energy storage in Li-ion batteries and their specific capacity was evaluated by Cyclic Voltammetry (CV), Electrochemical Impedance Spectroscopy (EIS) and Charge-Discharge curves. The nanostructures that presented better electrochemical properties and superior behaviour as anode in lithium-ion batteries were those synthesized with  $H_2O_2$  as a complexing agent. This sample presents lower resistance to charge transfer and better behaviour during the cycling process, their specific capacity values during discharge and charge  $318 \text{ mAh}\cdot\text{g}^{-1}$  and  $310 \text{ mAh}\cdot\text{g}^{-1}$ , respectively.

## 1. Introduction

Rechargeable lithium-ion (Li-ion) batteries are commonly employed in compact electronic devices and are contemplated the most promising power source for electric vehicles due to their long service life and high energy density. A lithium-ion battery involves two electrodes, the anode which is negatively charged and the cathode, which is positively charged, an electrolyte and a separator between both electrodes and the electrolyte.

The material from which the anode is made plays an important part in the function and capacity of the battery. Think about their excellent electrochemical reversibility and high specific capacitance, transition metal oxides are a potential supercapacitor material.  $WO_3$  is an n-type transition metal oxide and is a possible candidate for several applications such as gas sensors, electrochromic devices, microelectronics, supercapacitors, etc. Various methods have been used for the synthesis of  $WO_3$  nanostructures, but electrochemical anodization has attracted much attraction because it is quite a simple and quick preparation technique.

The reaction of  $WO_3$  with ligands or complexing agents (such as citric acid, hydrogen peroxide or polycarboxylic acids) can be applied to modify  $WO_3$  nanostructures, thus providing a wide range of opportunities to achieve new morphologies and improved properties.

Therefore, in this work, the influence of the ligand on the electrochemical behaviour of the formed nanostructures that will act as the anode in the batteries has been investigated. All electrodes have been characterized morphologically by FE-SEM microscopy, structurally by Raman Spectroscopy, electrochemically by EIS and finally, their behaviour as an anode in lithium-ion batteries was evaluated by Charge-Discharge curves and Cyclic Voltammeteries.

## 2. Experimental procedure

### 2.1. Nanostructures synthesis and characterization

Nanostructures of  $\text{WO}_3$  were synthesized using two different complexing agents ( $\text{H}_2\text{O}_2$  and citric acid) following the methodology explained in previous work (Cifre-Herrando *et al.*, 2022). The morphology of the samples was analyzed by employing FE-SEM (Zeiss Ultra 55 Scanning Electron Microscope) at an acceleration potential of 2 kV. The crystal structure of the samples was examined with a confocal Raman laser microscope (Witec alpha 300 R confocal Raman microscope) using a neon laser of 488 nm and 420  $\mu\text{W}$  power in a range of 0 to 2000  $\text{cm}^{-1}$ . Electrochemical analyses were realized using a three-electrode system: Ag/AgCl (3 M KCl) as a reference electrode, a platinum tip as a counter electrode and the nanostructures as a working electrode. Photoelectrochemical impedance spectroscopy (PEIS) measurements were realized by applying 1 V Ag/AgCl with an amplitude of 10 mV in the frequency range of  $10^5$  Hz to 0.01 Hz using an Autolab PGSTAT302N potentiostat (Metrohm). In all photoelectrochemical analyses, 0.1 M  $\text{H}_2\text{SO}_4$  is used as the electrolyte to ensure the stability of the nanostructures (Lassner and Schubert, 1999).

### 2.2. Energy storage application

To analyze the electrochemical behaviour of the nanostructures as anode in lithium-ion batteries, Cyclic Voltammetry, Charge-Discharge tests, and Electrochemical Impedance Spectroscopy were performed. To carry out these three tests, two-electrode cell configuration was employed. This cell consists of an anode (the  $\text{WO}_3$  nanostructures previously synthesized), a cathode (a lithium sheet) and the electrolyte (1 M  $\text{LiPF}_6$  in solution, a nonaqueous solution of dimethyl carbonate, and ethylene carbonate with a volume ratio of 1:1). In addition, fibreglass was used as separators. These three components were assembled in a glove box with an argon atmosphere. An Autolab PGSTAT302N potentiostat was used for the electrochemical tests. First, Cyclic Voltammetry was performed on both samples with a scan rate of  $0.5 \text{ mV}\cdot\text{s}^{-1}$  and range potential between 0.01 and 4.0V. After that, Charge-Discharge tests were carried out using a range potential of 0.01–4 V versus  $\text{Li}/\text{Li}^+$  and a current density of  $100 \text{ mA}\cdot\text{g}^{-1}$ . Finally, the EIS tests were performed using a frequency range of 0.1–10 kHz and a signal perturbation with an amplitude of 10 mV.

## 3. Results and discussion

### 3.1. Nanostructures characterization

The electrodes were morphologically analyzed by FE-SEM. Figure 1 shows the FE-SEM images of the  $\text{WO}_3$  samples synthesized with different electrolytes (a) 0.05 M  $\text{H}_2\text{O}_2$  and (b) 0.1 M citric acid and annealed at 600  $^\circ\text{C}$ .

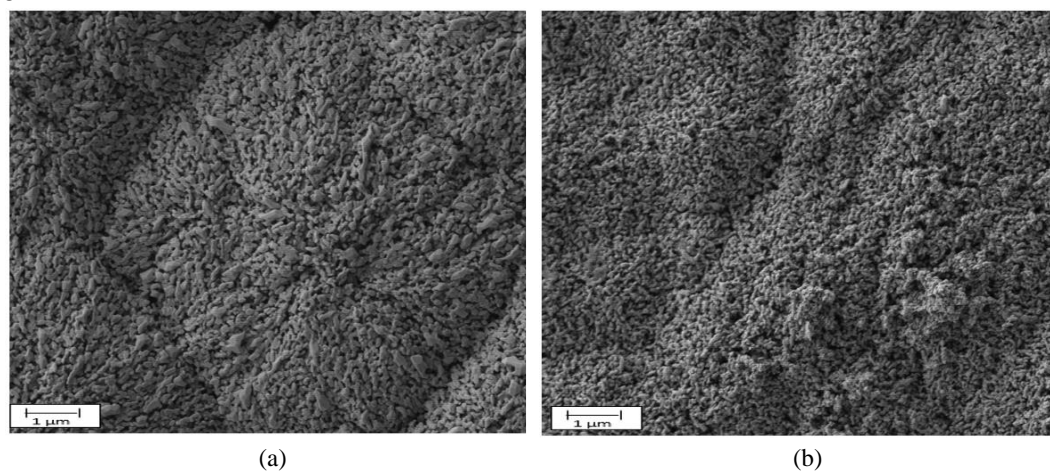


Figure 1. FE-SEM images at 10 000x magnification of the  $\text{WO}_3$  samples synthesized with different electrolytes and annealed at 600  $^\circ\text{C}$  (a) 0.05 M  $\text{H}_2\text{O}_2$  and (b) 0.1 M citric acid.

It can be seen that, in both cases, the morphology obtained was similar, obtaining a homogeneous layer of small-sized nanoparticles. This morphology is due to the degree of dehydration reached by the nanostructures after the annealing treatment at 600 °C after their synthesis (Cifre-Herrando *et al.*, 2022). Furthermore, the similarity in morphology between the two nanostructures is explained by the fact that both electrolytes act as bidentate complexing agents and the process of nanostructure synthesis is the same (Fernández-Domene *et al.*, 2021). The difference between the two electrolytes is minimal, although in the nanostructures obtained with H<sub>2</sub>O<sub>2</sub>, the mountain shape of the nanorods appears slightly more compact than in those obtained with citric acid. Raman spectra were used to study the effect of the electrolyte used in the synthesis of nanostructures on their crystalline structure. Figure 2 shows the Raman spectrum for the samples synthesized with 0.05 M H<sub>2</sub>O<sub>2</sub> and 0.1 M citric acid where the shape of the spectra for both samples is similar. In both cases, the characteristic peaks of the monoclinic WO<sub>3</sub> phase appear: 125 cm<sup>-1</sup>, 273 cm<sup>-1</sup>, 327 cm<sup>-1</sup>, 704 cm<sup>-1</sup> and 804 cm<sup>-1</sup>. The sharpest peaks appear at 707 and 805 cm<sup>-1</sup>, which are associated with the W-O stretching and bending modes. In addition, the other characteristic peaks of the monoclinic WO<sub>3</sub> (125 cm<sup>-1</sup>, 273 cm<sup>-1</sup>, 327 cm<sup>-1</sup>) which also occur, although less pronouncedly, are associated with the O-W-O bending modes, indicating the existence of crystalline tungsten oxide and oxygen vacancies and therefore, high levels of crystallinity and dehydration (Yoon *et al.*, 2014; Park *et al.*, 2015).

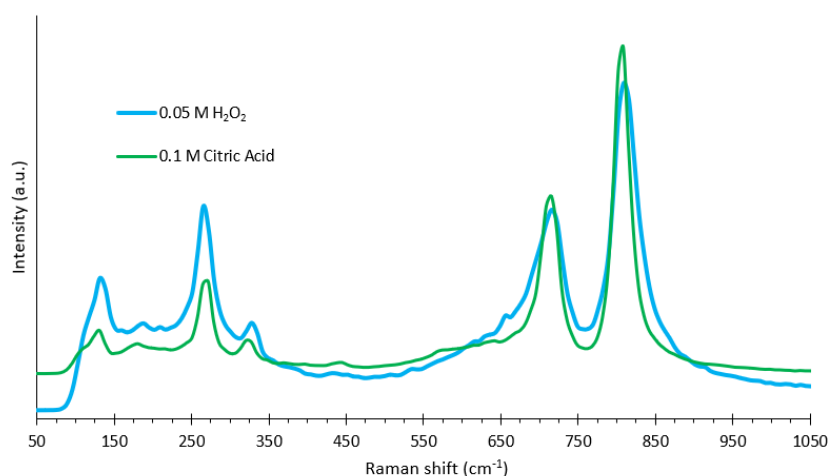


Figure 2. Raman spectra of WO<sub>3</sub> samples synthesized with 0.05 M H<sub>2</sub>O<sub>2</sub> and 0.1 M citric acid.

Electrochemical impedance spectroscopy (EIS) tests were performed in both nanostructures in order to study the influence of the complexing agent on the electrochemical phenomena that occur in WO<sub>3</sub> nanostructures. Figure 3 shows Nyquist diagrams and Bode plots obtained from EIS tests and the equivalent circuit obtained to quantitatively analyze EIS results.

Nyquist diagram (Figure 3 a) is related to the charge-transfer processes of the electron-hole pairs. As can be observed in the Nyquist plot, a semicircle appears for both electrolytes. The amplitude of the semicircle is referred to the charge transfer resistance from the WO<sub>3</sub> electrode to the electrolyte, the smaller the semicircle width, the better the electrochemical response (Roselló-Márquez *et al.*, 2022). As it can be seen in Figure 3a, the semicircle for citric acid is slightly lower than for H<sub>2</sub>O<sub>2</sub>, consequently, the electrochemical properties are also slightly better for citric acid than for H<sub>2</sub>O<sub>2</sub>. From Bode phase diagrams (Figure 3b), a wide peak can be seen for both electrolytes, indicating the superposition of two individual peaks. It can be appreciated that the phase angle is similar for both electrolytes, indicating similar resistance and therefore similar electrochemical properties.

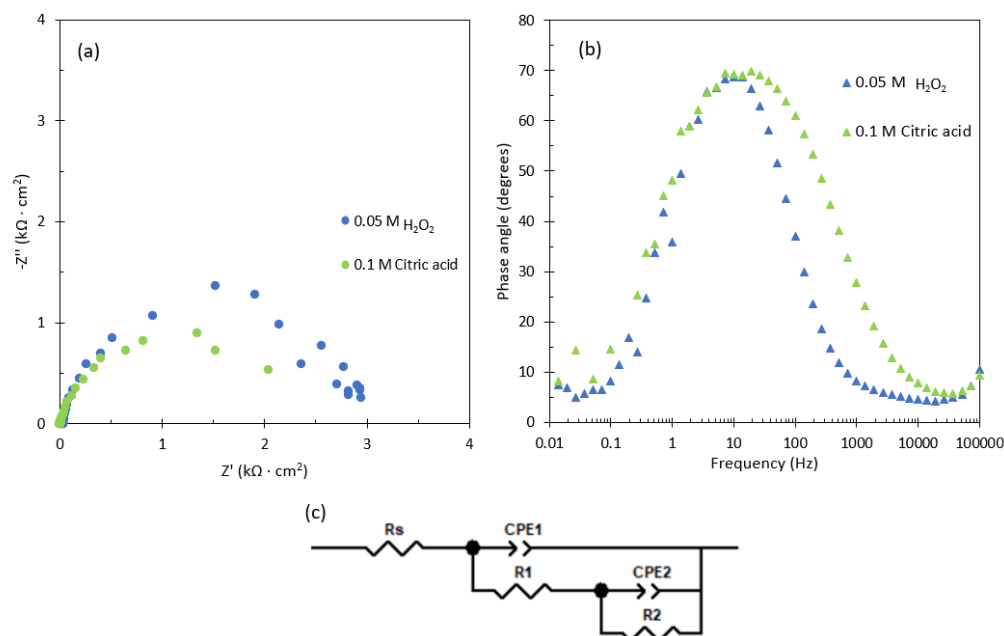


Figure 3. EIS plots. (a) Nyquist impedance plots and (b) Bode plots of the nanostructures synthesized with 0.05 M  $H_2O_2$  and 0.1 M citric acid (c) Equivalent circuit.

### 3.2. Energy storage tests

To evaluate the electrochemical behaviour of both samples, Cyclic Voltammetry was performed in the first place. Figure 4 shows the result of these voltammetry's, where in the first cycle two reduction peaks are observed (at approximately 0.6 V and 1.4 V) and two more oxidation peaks (at approximately 1.25 V and 2.6 V). The peaks that appear in the reduction zone refer to the formation of  $Li_2O$  (according to equation 1), while the peaks in the oxidation zone refer to the lithium extraction process (according to equation 2) (Siddique *et al.*, 2021). The disappearance of the reduction peak at 0.6 V in the next two cycles in both cases suggests the formation of a solid electrolyte interphase (SEI) layer during the first cycle that produces a specific capacitance reduction. Furthermore, as this peak is more pronounced in the case of the sample synthesized with citric acid, it can be stated that the irreversible reduction in capacity, in this case, will be greater (Li *et al.*, 2016). Regarding the oxidation peaks, the peak that appears at 1.25 V remains in all cycles when  $H_2O_2$  is used as a complexing agent, indicating that the reaction is reversible, while in the sample synthesized with citric acid, this peak disappears, showing that the extraction of lithium reaction is irreversible and therefore decreases the specific capacity of the battery during the following cycles.

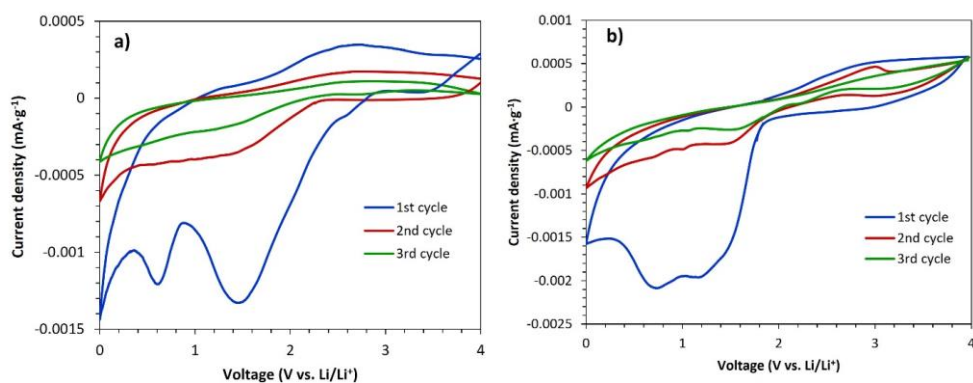
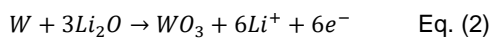
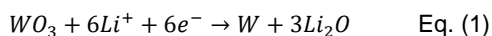


Figure 4. Cycle voltammograms curves of  $WO_3$  nanostructures synthesized with a)  $H_2O_2$  and b) citric acid.

The results obtained after carrying out the first cycle of the Charge-Discharge test of both samples are shown in Figure 5. The shape of both discharge curves is similar, where two sections with different slopes and a plateau are observed. The plateau observed in both cases is associated with the formation of W and  $\text{Li}_2\text{O}$  (Equation 1) and the growth of an SEI layer (Tang, Tse and Liu, 2016; Roselló-Márquez *et al.*, 2022)

However, the value of specific capacity is different in both cases. The sample synthesized with citric acid as a complexing agent has a higher specific capacity during the first discharge, being  $611 \text{ mAh}\cdot\text{g}^{-1}$ , while the value corresponding to the sample synthesized with  $\text{H}_2\text{O}_2$  is  $318 \text{ mAh}\cdot\text{g}^{-1}$ .

On the other hand, analysing the charge curves, it can be observed that the samples synthesized with  $\text{H}_2\text{O}_2$  achieve a higher specific capacity ( $310 \text{ mAh}\cdot\text{g}^{-1}$ ) than those synthesized with citric acid ( $50 \text{ mAh}\cdot\text{g}^{-1}$ ), and therefore, it indicates that these nanostructures will withstand more charge and discharge cycles, presenting a better behaviour as an anode in lithium-ion battery.

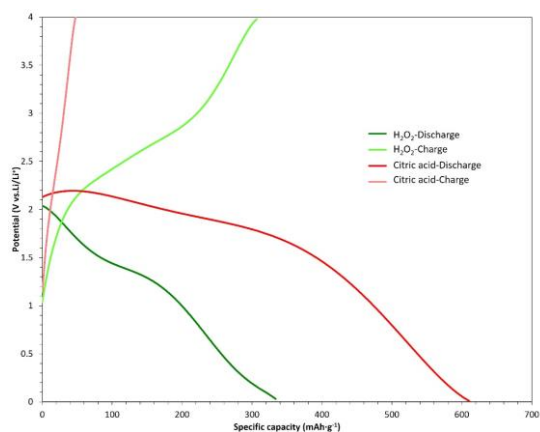


Figure 5. Charge/discharge curves of  $\text{WO}_3$  nanostructures synthesised with  $\text{H}_2\text{O}_2$  and citric acid in the 0.01–4 V versus  $\text{Li}/\text{Li}^+$  range voltage at  $100 \text{ mA g}^{-1}$  current density.

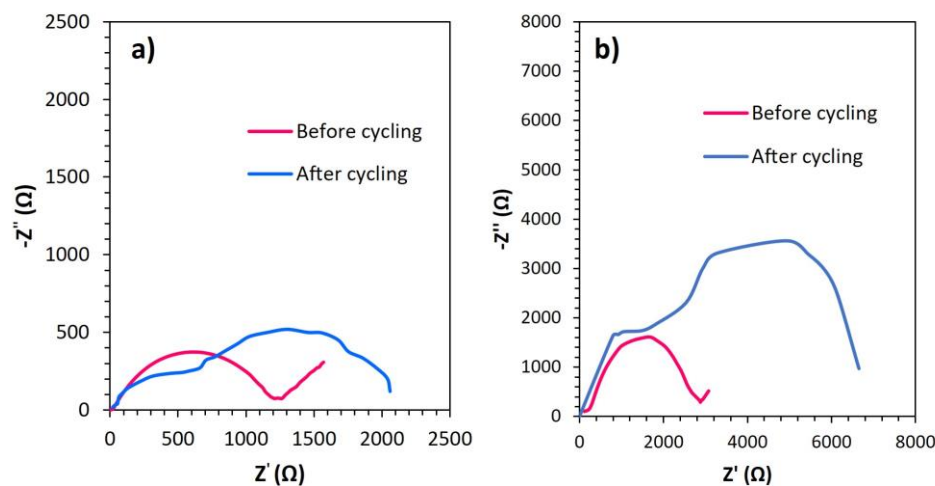


Figure 6. Nyquist plots before and after cycling  $\text{WO}_3$  nanostructures obtained with a)  $\text{H}_2\text{O}_2$  and b) citric acid.

Finally, EIS tests were carried out to verify which sample showed the lowest charge transfer resistance and the best behaviour as an anode in lithium-ion batteries. In both cases, these impedances were performed before and after the cycling process to see which sample supports in a best way this process. As shown in Figure 6, in both cases before cycling, the samples present a semicircle with an inclined slope that refers to the diffusion of lithium ions (Zheng *et al.*, 2018). The width of this semicircle refers to the charge transfer resistance (Faraji, Hassanzadeh and Mohseni, 2017) and it can be observed that this value is lower for the nanostructures obtained with  $\text{H}_2\text{O}_2$ .

Analysing the spectrum after submitting them to the cycling process (after doing 50 charge and discharge cycles), the appearance of a second semicircle and a greater resistance in both cases are observed, but this is even greater in the case of the sample obtained with citric acid. Therefore, it is again concluded that these nanostructures present worse behaviour as anode in lithium-ion batteries.

#### 4. Conclusions

The objective of this study was to study the effect of the complexing agent in the synthesis of WO<sub>3</sub> nanostructures to use them as anode in lithium-ion batteries. From the characterization results, it can be affirmed that the morphology and crystallinity of the nanostructures is similar. However, electrochemical results showed that nanostructures synthesized with H<sub>2</sub>O<sub>2</sub> exhibit better behavior during the cycling process and show an improved electron transport capacity during the Li<sup>+</sup> insertion/de-insertion process. In summary, WO<sub>3</sub> nanostructures synthesized with H<sub>2</sub>O<sub>2</sub> are interesting to be used as anode in lithium-ion batteries.

#### Acknowledgments

Authors would like to express their gratitude to AEI (PID2019-105844RB-I00/AEI/10.13039/501100011033) for the financial support. M. Cifre-Herrando thank Ministerio de Universidades for the concession of the pre-doctoral grant (FPU19/02466). G. Roselló-Márquez also thanks the UPV for the concession of a post-doctoral grant (PAID-10-21) and for the grant to promote postdoctoral research at the UPV (PAID.-PD-22). Finally, project co-funded by FEDER operational programme 2014-2020 of Comunitat Valenciana (IDIFEDER/18/044) is acknowledged.

#### References

- Cifre-Herrando, M. Roselló-Márquez, G. García-García, D.M. (2022) 'Degradation of Methylparaben Using Optimal WO<sub>3</sub> Nanostructures: Influence of the Annealing Conditions and Complexing Agent', *Nanomaterials*, 12(23). doi: 10.3390/nano12234286.
- Faraji, M., Hassanzadeh, A. and Mohseni, M. (2017) 'Interlaced WO<sub>3</sub>-carbon nanotube nanocomposite electrodeposited on graphite as a positive electrode in vanadium redox flow battery', *Thin Solid Films*, 642(September), pp. 188–194. doi: 10.1016/j.tsf.2017.09.044.
- Fernández-Domene, R. M. Roselló-Marquez, G., Sánchez-Tovar, R., Cifre-Herrando, M. García-Antón, J. (2021) 'Synthesis of WO<sub>3</sub> nanorods through anodization in the presence of citric acid: Formation mechanism, properties and photoelectrocatalytic performance', *Surface and Coatings Technology*, 422(June). doi: 10.1016/j.surfcoat.2021.127489.
- Lassner, E. and Schubert, W.-D. (1999) *Tungsten: properties, chemistry, technology of the elements, alloys, and chemical compounds*. Springer Science & Business Media.
- Li, P. Li, X. Wang, M. Foz, T. Zhang, Q., Zhou Y. (2016) 'Correlations among structure, composition and electrochemical performances of WO<sub>3</sub> anode materials for lithium ion batteries', *Electrochimica Acta*, 192, pp. 148–157. doi: 10.1016/j.electacta.2016.01.199.
- Park, S. K., Lee, H.J, Park, H.S. (2015) 'Hierarchically structured reduced graphene oxide/WO<sub>3</sub> frameworks for an application into lithium ion battery anodes', *Chemical Engineering Journal*, 281, pp. 724–729. doi: <https://doi.org/10.1016/j.cej.2015.07.009>.
- Roselló-Márquez, G. García-García, D.M, Cifre-Herrando, M.C, Blaco-Tamarit, E., García-Antón, J.(2022) 'Facile preparation of electrodes based on WO<sub>3</sub> nanostructures modified with C and S used as anode materials for Li-ion batteries', *Journal of the American Ceramic Society*, (October), pp. 1–17. doi: 10.1111/jace.18910.
- Siddique, F. Fareed, S., Jamil, A., Afsar, M.F., Rafiq, M. A., Sher, F. (2021) 'Synthesis of randomly oriented self-assembled WO<sub>3</sub> and WO<sub>3</sub>-WS<sub>2</sub> nanoplates for selective oxygen sensing', *Journal of the Australian Ceramic Society*, 57(4), pp. 1231–1240. doi: 10.1007/s41779-021-00622-0.
- Tang, Z. K., Tse, J. S. and Liu, L. M. (2016) 'Unusual Li-Ion Transfer Mechanism in Liquid Electrolytes: A First-Principles Study', *Journal of Physical Chemistry Letters*, 7(22), pp. 4795–4801. doi: 10.1021/acs.jpcllett.6b02351.
- Yoon, S. Woo, S., Jung K., Song, H. (2014) 'Conductive surface modification of cauliflower-like WO<sub>3</sub> and its electrochemical properties for lithium-ion batteries', *Journal of Alloys and Compounds*, 613, pp. 187–192. doi: <https://doi.org/10.1016/j.jallcom.2014.06.010>.
- Zheng, M., Tang, H., Li, L., Hu, Q., Zhang, L., Xue, H., Pang, H. (2018) 'Hierarchically Nanostructured Transition Metal Oxides for Lithium-Ion Batteries', *Advanced Science*, 5(3). doi: 10.1002/advs.201700592.